CrossMark

ORIGINAL PAPER

Manifestations of intermittency in unidirectionally coupled Pierce diodes on different time scales

**O. I. Moskalenko · M. O. Zhuravlev ·
A. A. Koronovskii · A. E. Hramov**

Abstract Intermittent behavior in unidirectionally coupled Pierce diodes being a classical model of spatially extended beam–plasma systems on different time scale is studied. Depending on the value of the strength of coupling between interacting systems and selected time scale, the ring intermittency, the eyelet intermittency or coexistence of both of them are shown to be observed.

Intermittency is one of the widespread phenomena in nonlinear science [1–8]. It is observed in flow systems, discrete maps and spatially distributed media. It is one of the classical scenarios of the transition to chaos and can also take place near the boundaries of different types of chaotic synchronization [9–15]. Intermittency manifests itself on the different time scales. In particular, in the phase synchronized flow chaotic systems the ring intermittency is observed on the boundary time

O. I. Moskalenko (✉) · A. A. Koronovskii
Saratov State University, Astrakhanskaya, 83, Saratov,
Russia 410012
e-mail: o.i.moskalenko@gmail.com

M. O. Zhuravlev · A. E. Hramov
Saratov State Technical University, Politehnicheskaya, 77,
Saratov, Russia 410054

scales [16], whereas near the boundary of the phase synchronization depending on the selected time scales the ring intermittency, the eyelet intermittency or coexistence of both types of intermittency mentioned above can take place [17]. Each type of the intermittency is characterized by its own statistical characteristics determined by the mechanisms (which are also different for the distinct intermittencies) resulting in the intermittent dynamics. These statistical characteristics (the distributions of the laminar and turbulent phase lengths calculated for the fixed values of the control parameters, the dependence of the mean length of the laminar phases on the control parameter and/or parameters of analysis) are used frequently to classify the type of intermittent behavior observed in the experimental or theoretical studies.

Spatially extended nonlinear systems (including active media, complex networks and living objects) are also known to exhibit intermittent behavior [3,5, 6,18–21]. At the same time, the most part of known papers is devoted to the consideration of the coupled-map lattices, complex networks or dynamics of spatially distributed active media, whereas transitions from the asynchronous dynamics to different types of chaotic synchronization in such systems have not been studied in detail now. As an exception, one can refer to the papers [14,15] where intermittent phase and generalized synchronization has been studied, with the mechanisms of the synchronous regime arising and statistical characteristics of intermittency being the same as in the case of the systems with a small number of degrees of

freedom. Obviously, one can expect that for the spatially extended systems the analysis of their behavior on different time scales in dependence on the coupling parameter, similarly to the analogous studies of the systems with a small number of degrees of freedom, may reveal the interesting phenomena and generalities. Nevertheless, the analogous investigations in spatially extended media have not been performed so far. Therefore, in the present paper we analyze the manifestations of intermittency in spatially distributed systems on different time scales of observation.

As an object of the research, we consider two unidirectionally coupled hydrodynamical models of Pierce diodes (indices "1" and "2" correspond to the drive and response systems, respectively) whose dynamics in the dimensionless form is given by

$$\frac{\partial^2 \varphi_{1,2}}{\partial x^2} = -\alpha_{1,2}^2 (\rho_{1,2} - 1), \qquad (1)$$
$$\frac{\partial \rho_{1,2}}{\partial t} = -\frac{\partial (\rho_{1,2} v_{1,2})}{\partial x},$$
$$\frac{\partial v_{1,2}}{\partial t} = -v_{1,2} \frac{\partial v_{1,2}}{\partial x} + \frac{\partial \varphi_{1,2}}{\partial x},$$

where $\alpha_1 = 2.858\pi$ and $\alpha_2 = 2.860\pi$ are the control parameters, $0 \leq x \leq 1$, $\varphi_{1,2}(x, t)$ are potentials of the electric field, and $\rho_{1,2}(x, t)$ and $v_{1,2}(x, t)$ are the densities and velocities of the electron beam, respectively [22,23]. The boundary conditions on the left boundary are specified by the constant ones

$$v_{1,2}(0, t) = 1, \quad \rho_{1,2}(0, t) = 1, \quad \varphi_{1,2}(0, t) = 0, \quad (2)$$

whereas on the right boundary of the systems they are modified in the following way

$$\begin{cases} \varphi_1(1, t) = 0, \\ \varphi_2(1, t) = \varepsilon(\rho_2(x = 1, t) - \rho_1(x = 1, t)), \end{cases} \qquad (3)$$

defining the unidirectional coupling between interacting systems [24]. Here ε denotes the strength of coupling between such systems.

To analyze the behavior of interacting Pierce diodes on different time scales of observation, we follow the time scale synchronization concept [25–27] and use the continuous wavelet transform [27,28]

$$W_{1,2}(s, t_0) = \frac{1}{\sqrt{s}} \int_{-\infty}^{+\infty} u_{1,2}(t) \psi^* \left(\frac{t - t_0}{s}\right) dt, \qquad (4)$$

with Morlet complex mother wavelet $\psi(\eta) = (1/\sqrt[4]{\pi})$ $\exp(j\Omega_0\eta)\exp\left(-\eta^2/2\right)$, $\Omega_0 = 2\pi$. Here $u_{1,2}(t)$ are time realization of the analyzed systems, and s is a time scale of observation. As signals $u_{1,2}(t)$ for Pierce diodes, we use the space charge densities $\rho_{1,2}(x = 0.2, t)$ registered in the fixed point $x = 0.2$ of the interaction space.

The use of complex wavelet basis allows to introduce into consideration the phases $\phi_{1,2}(s, t) = \arg W_{1,2}$ (s, t) for any time scale s. The efficiency of the Morlet wavelet function for introduction of the phases of time series of different nature (biological and electromagnetic signals) has been confirmed in the earlier studies [16,25,26,29–31]. If for the selected time scale the phase locking condition

$$|\phi_1(s, t) - \phi_2(s, t)| < 2\pi \qquad (5)$$

is satisfied, the time scale s can be considered as the synchronous one. The number of synchronous time scales depends both on the system itself and its control parameters. However, for any dynamical system the range of synchronous time scales expands with increase in the value of the coupling strength testifying the transition from the phase to lag synchronization regime [25,32].

In the phase synchronization regime, the system under study contains both synchronous and asynchronous time scales. They are delimited by so-called boundary time scales in which the intermittent behavior can be observed. Similar effects take place near the phase synchronization boundary. But due to the presence of intermittent behavior in such region on the boundary time scales of observation, the intermittency of intermittencies [17] should take place.

Let us define the characteristics of intermittency on different time scales both in the regime of phase synchronization and near its boundary in unidirectionally coupled Pierce diodes (1)–(3). To define the type of intermittency realized for the selected control parameter values, we use, first of all, the rotating plane method [16,17]. Due to such approach, the dynamics of interacting systems can be considered on the plane (ξ', η') rotating around the origin $(0, 0)$ according to the phase ϕ_1 of the first system

$$\begin{aligned} \xi' &= \xi_2 \cos \phi_1 + \eta_2 \sin \phi_1, \\ \eta' &= -\xi_2 \sin \phi_1 + \eta_2 \cos \phi_1, \end{aligned} \qquad (6)$$
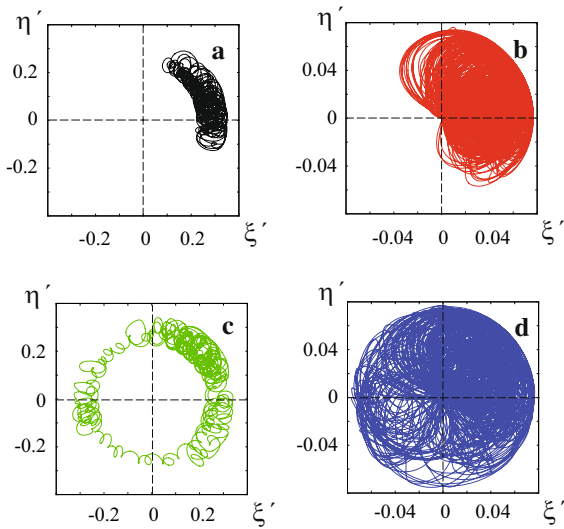
Fig. 1 (Color online) Phase trajectories of Pierce diodes on the rotating plane (ξ', η') for different values of the coupling strength ε and the time scale s: **a** the synchronous regime ($\varepsilon = 0.058$, $s = 4.0$), **b** the ring intermittency ($\varepsilon = 0.058$, $s = 2.7225$), **c** the eyelet intermittency ($\varepsilon = 0.00445$, $s = 4.0$), **d** the intermittency of eyelet and ring intermittencies ($\varepsilon = 0.00445$, $s = 2.7225$)

where $\xi_2 = \mathrm{Re}\,W_2(s, t)$, $\eta_2 = \mathrm{Im}\,W_2(s, t)$. Figure 1 illustrates the behavior of interacting Pierce diodes on the plane (6) for different values of the coupling strength ε and time scale of observation s. Figure 1a, b corresponds to the realization of the regime of phase synchronization in the system (1)–(3) ($\varepsilon = 0.058$). In such case on the main time scale of observation ($s = 4.0$, Fig. 1a), the trajectory on the rotating plane looks like a smeared fixed point which does not envelop the origin, whereas on the boundary time scale ($s = 2.7225$, Fig. 1b) it is represented by a similar point enveloping origin. In such case, the ring intermittency[13] should be realized. Near the phase synchronization boundary ($\varepsilon = 0.00445$), the trajectory on the rotating plane looks like a smeared limit cycle on the main time scale of observation ($s = 4.0$, Fig. 1c) which starts enveloping origin at consideration of the system on the boundary time scale ($s = 2.7225$, Fig. 1d). It is obvious that in the first case (Fig. 1c), the eyelet intermittency [12] should be observed in the system under study, whereas in the second one (Fig. 1d) the coexistence of eyelet and ring intermittencies should take place.

To verify the results obtained by means of the rotation plane approach, we analyze statistical characteristics of the fields of the synchronous behavior (laminar phases) in two unidirectionally coupled Pierce beam–plasma diodes on different time scales of observation. They are (1) the distribution of lengths of the laminar behavior for the fixed values of the system parameters and (2) the dependencies of the mean length of the laminar behavior on the coupling parameter (for the fixed time scale) and on the time scale (for the fixed coupling parameter). Ring and eyelet intermittencies are known to be characterized by an exponential distribution of the lengths of the phases of laminar behavior, but in the regime of eyelet intermittency it takes place only for relatively large values of lengths (see [33,34]). In other words, the distribution of the lengths of the laminar phases in the eyelet intermittency regime obeys an exponential law

$$p_1(\tau) = \frac{1}{K T_1} \exp\left(-\frac{\tau}{T_1}\right) \qquad (7)$$

where $K = \exp\left(-\dfrac{x}{T_1}\right)$, T_1 is a mean length of the laminar phases for eyelet intermittency, x is a minimal value of the laminar phase length for which distribution obeys an exponential law [34,35], whereas in the regime of ring intermittency it can be written in the following form

$$p_2(\tau) = \frac{1}{T_2} \exp\left(-\frac{\tau}{T_2}\right) \qquad (8)$$

where T_2 is the mean length of the laminar phases for ring intermittency [13]. Taking into account the peculiarity of the laminar phase length distribution for eyelet intermittency (7) which has not been taken into account in the previous works (see, e.g., [17,34,36]), on the basis of the common theory of coexistence of two different types of intermittent behavior in nonlinear systems proposed in [17], one can deduce the refined distribution of the laminar phase lengths for the regime of intermittency of eyelet and ring intermittencies. Having substituted the probability densities (7) and (8) for $p_{1,2}(\tau)$ into relation

$$p(\tau)$$
$$= \frac{1}{T_1 + T_2}\left[\int_\tau^\infty \frac{ds}{s} \int_\tau^\infty [p_1(l)p_2(s)T_2 + p_1(s)p_2(l)T_1]\,dl\right.$$
$$\left. + \int_\tau^\infty \left(1 - \frac{\tau}{s}\right)[p_1(\tau)p_2(s)T_2 + p_1(s)p_2(\tau)T_1]\,ds\right]$$

reported in [17] for the intermittency of intermittencies and made its further simplifications, one can obtain the refined distribution of the laminar phase lengths

$$
p(\tau) = 2\exp\left(\frac{x-\tau}{T_1} - \frac{\tau}{T_2}\right)\left(T_1^2 - T_1 e^{\tau/T_1}(\tau - T_2)\Gamma\right.
$$

$$
\times \left(0, \frac{\tau}{T_1}\right) - T_2(\tau - T_1)
$$

$$
\times e^{\tau/T_2}\Gamma\left(0, \frac{\tau}{T_2}\right) + T_2^2\right) \Big/
$$

$$
\left(T_1 T_2\left(2x\mathrm{Ei}\left(-\frac{x}{T_1}\right)e^{x\left(\frac{1}{T_1} - \frac{1}{T_2}\right)}\right.\right.
$$

$$
+ 2x\mathrm{Ei}\left(-\frac{x}{T_2}\right) + 2T_1 e^{-\frac{x}{T_2}}
$$

$$
- 2T_1 e^{x/T_1}\ln\left(\frac{T_1 + T_2}{T_1}\right)
$$

$$
+ T_1 e^{x/T_1}\ln\left(\frac{1}{T_1} + \frac{1}{T_2}\right)
$$

$$
+ 2T_1 e^{x/T_1}\ln(T_2) - T_1 e^{x/T_1}
$$

$$
\times \ln\left(\frac{T_1 T_2}{T_1 + T_2}\right) + 2T_2 e^{x/T_1}\ln(T_1)
$$

$$
+ T_2 e^{x/T_1}\ln\left(\frac{1}{T_1} + \frac{1}{T_2}\right) - 2T_2 e^{x/T_1}
$$

$$
\times \ln\left(\frac{T_1 + T_2}{T_2}\right) - T_2 e^{x/T_1}
$$

$$
\ln\left(\frac{T_1 T_2}{T_1 + T_2}\right) + 2T_2 e^{-\frac{x}{T_2}}\right)\right)
\tag{9}
$$

where $\Gamma(a, z)$ is incomplete Γ-function and $\mathrm{Ei}(z)$ is an exponential integral function.

To show the validity of obtained relation and to prove the existence of different types of intermittency in unidirectionally coupled Pierce diodes, we have calculated numerically the distributions of the laminar phase lengths for the regimes shown in Fig. 1b–d (with the same values of the criticality parameters) and compare them with the theoretical relations (7)–(9). These distributions are shown in Fig. 2. Curve *1* corresponds to the ring intermittency regime, curve *2* refers to the regime of eyelet intermittency, whereas curve *3* reflects the coexistence of eyelet and ring intermittencies. It is clearly seen that in all considered cases the numerical data are in a good agreement with the results of theoretical predictions that confirm realization of the different types of intermittency including the coexistence of them in unidirectionally coupled Pierce diodes on the different time scales of observation.
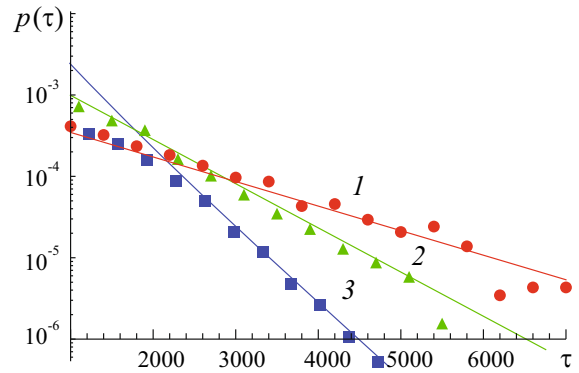

Fig. 2 (Color online) Distributions of the lengths of the laminar phases in interacting Pierce diodes for different values of the coupling strength ε and the time scale s: curve *1*—the ring intermittency ($\varepsilon = 0.058$, $s = 2.7225$), curve *2*—the eyelet intermittency ($\varepsilon = 0.00445$, $s = 4.0$), curve *3*—the intermittency of eyelet and ring intermittencies ($\varepsilon = 0.00445$, $s = 2.7225$). The numerical results are marked by *points*, whereas their theoretical approximations are shown by *lines*. The approximation parameters are the following: $T_1 = 1332.51$, $T_2 = 1439.16$, $x = 400$

As we have mentioned above, an additional evidence of the presence of the different types of intermittency in unidirectionally coupled Pierce diodes is the behavior of the mean length of the laminar phases with the criticality parameter variation. In the regime of eyelet intermittency, it obeys relation

$$
T_1(\varepsilon) = A\exp\kappa(\varepsilon_c - \varepsilon)^{-1/2},
\tag{10}
$$

where ε_c is a critical value of the coupling parameter corresponding to the onset of the phase synchronization, A and κ are the parameters of approximation [2,36,37]. In the ring intermittency regime, such dependence is the following

$$
T_2(s) = T_0\left(1 - \frac{1}{\ln(1 - \Pi(s))}\right)
\tag{11}
$$

where T_0 is a mean length of the laminar phases for the time scale bounding the region of ring intermittency and $\Pi(s)$ is the probability of detection of turbulent motion in the fixed time of the observation [13,16]. Taking into account the obtained relation for probability distribution (9) in the regime of coexistence of eyelet and ring intermittencies, one can obtain the relation for the mean length of the laminar phases for this regime. Having substituted Eq. (9) for $p(\tau)$ into the definition of the mean value
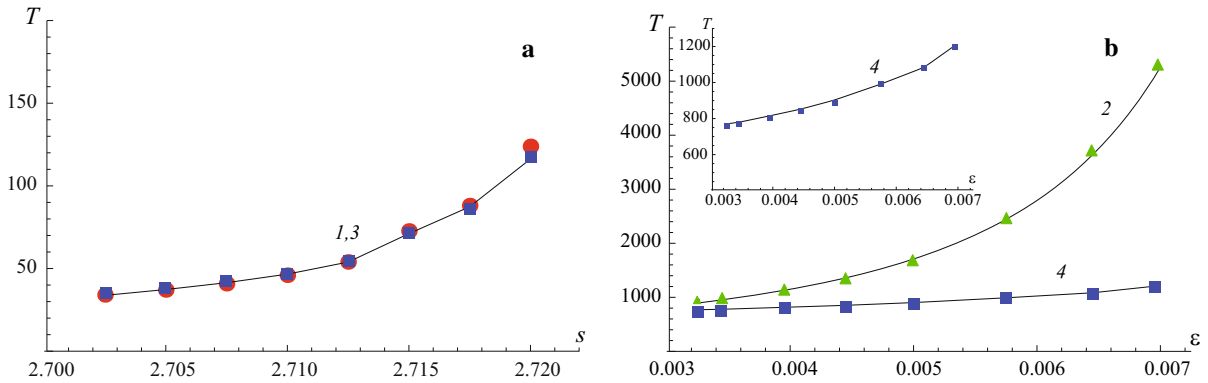
Fig. 3 (Color online) **a** Dependence of the mean length of the laminar phases on the time scale s for fixed coupling parameters in the regimes of ring intermittency ($\varepsilon = 0.058$, curve *1*) and intermittency of eyelet and ring intermittencies ($\varepsilon = 0.00445$, curve *3*) and their theoretical approximations. **b** Dependencies of the mean length of the laminar phases on the coupling parameter ε for fixed time scales in the regimes of eyelet intermittency ($s = 4.0$, curve *2*) and intermittency of eyelet and ring inter-

mittencies ($s = 2.7225$, curve *4*) and their theoretical approximations. The numerical data are marked by *points*, and their theoretical approximations by laws (10)–(13) are shown by *solid lines*. In the frame, the enlarged part of the curve *4* is shown. The parameters of approximations are the following: $A = 3.7$, $\kappa = 0.5133$, $\varepsilon_c = 0.012$, $T_0 = 13.5$, and the probability $p(s)$ is assumed to be linear

$$T = \int_x^\infty \tau p(\tau) \mathrm{d}\tau, \tag{12}$$

one can obtain the relation for the mean length of the laminar phases for the regime of intermittency of eyelet and ring intermittencies in the form

$$
\begin{aligned}
T(\varepsilon, s) = {} & 2e^{-\frac{x}{T_2}} \Bigg(\left(T_1^2 + T_1 x + x^2 \right) e^{x/T_2} \mathrm{Ei}\left(-\frac{x}{T_2} \right) \\
& + T_1^2 \left(-e^x \left(\frac{1}{T_1} + \frac{1}{T_2} \right) \right) \\
& \times \mathrm{Ei}\left(-\frac{(T_1 + T_2)x}{T_1 T_2} \right) \\
& + e^{x/T_1} \left(T_2^2 + T_2 x + x^2 \right) \mathrm{Ei}\left(-\frac{x}{T_1} \right) \\
& - T_2^2 e^{x\left(\frac{1}{T_1} + \frac{1}{T_2} \right)} \mathrm{Ei}\left(-\frac{(T_1 + T_2)x}{T_1 T_2} \right) \\
& + 2T_1 T_2 + T_1 x + T_2 x \Bigg) \Bigg/ \\
& \left(2x\,\mathrm{Ei}\left(-\frac{x}{T_1} \right) e^{x\left(\frac{1}{T_1} - \frac{1}{T_2} \right)} \right. \\
& + 2x\,\mathrm{Ei}\left(-\frac{x}{T_2} \right) \\
& + 2T_1 e^{-\frac{x}{T_2}} - 2T_1 e^{x/T_1} \ln\left(\frac{T_1 + T_2}{T_1} \right) \\
& + T_1 e^{x/T_1} \ln\left(\frac{1}{T_1} + \frac{1}{T_2} \right) + 2T_1 e^{x/T_1}
\end{aligned}
$$

$$
\begin{aligned}
& \times \ln(T_2) - T_1 e^{x/T_1} \ln\left(\frac{T_1 T_2}{T_1 + T_2} \right) \\
& + 2T_2 e^{x/T_1} \ln(T_1) + T_2 e^{x/T_1} \ln\left(\frac{1}{T_1} + \frac{1}{T_2} \right) \\
& - 2T_2 e^{x/T_1} \ln\left(\frac{T_1 + T_2}{T_2} \right) \\
& - T_2 e^{x/T_1} \ln\left(\frac{T_1 T_2}{T_1 + T_2} \right) + 2T_2 e^{-\frac{x}{T_2}} \Bigg)
\end{aligned}
\tag{13}
$$

where the values $T_{1,2}$ and x can be obtained numerically for the regimes when the only one type of intermittent behavior should exist [17] [relations (10) and (11), respectively]. Figure 3 illustrates the numerically obtained dependencies of the mean lengths of the laminar phases on the time scale of observation (*a*) and the coupling parameter (*b*) and their theoretical approximations by the laws (10)–(13). As in Fig. 2, the curve *1* corresponds to the ring intermittency regime, curve *2* refers to the eyelet one and curves *3, 4* satisfy for the regime of intermittency of eyelet and ring intermittencies. It is clearly seen that in all considered cases the numerically obtained data are in a good agreement with the theoretical fits. Moreover, it is clearly seen that curves *1, 3* in Fig. 3a are almost coincident with each other, with the mentioned peculiarity being valid for both numerical and theoretical results. Such situation is connected with the fact that the lengths of the lami-

nar phases associated with the eyelet intermittency are extremely large in comparison with the last one associated with the ring intermittency regime. Therefore, the most part of the turbulent spikes in the regime of intermittency of intermittencies is associated with the ring intermittency and curves *1, 3* looks like almost identical.

So, as in the flow systems in the spatially extended systems described by the equations of unidirectionally coupled hydrodynamical models of Pierce diodes depending on the value of the coupling strength and time scale the different types of intermittency can be observed. In particular, in the regime of the phase synchronization on the boundary time scale of observation the ring intermittency takes place. Near the boundary of such regime depending on the time scale of observation, the eyelet intermittency or coexistence of eyelet and ring intermittencies can be realized. The found effect possess a high degree of generality. One can expect that such kind of behavior could be observed in variety of real systems (including the physical, radiotechnical and physiological ones) described in terms of both the systems with the small number of degrees of freedom and spatially extended media.

References

1. Perez Velazquez, J.L., et al.: Type III intermittency in human partial epilepsy. Eur. J. Neurosci. **11**, 2571–2576 (1999)
2. Boccaletti, S., Allaria, E., Meucci, R., Arecchi, F.T.: Experimental characterization of the transition to phase synchronization of chaotic CO_2 laser systems. Phys. Rev. Lett. **89**(19), 194101 (2002)
3. Cabrera, J.L., Milnor, J.: On-off intermittency in a human balancing task. Phys. Rev. Lett. **89**(15), 158702 (2002)
4. Manffra, E.F., Caldas, I.L., Viana, R.L., Kalinowski, H.J.: Type-I intermittency and crisis-induced intermittency in a semiconductor laser under injection current modulation. Nonlinear Dyn. **27**(2), 185–195 (2002)
5. Hramov, A.E., Koronovskii, A.A., Midzyanovskaya, I.S., Sitnikova, E., Rijn, C.M.: On-off intermittency in time series of spontaneous paroxysmal activity in rats with genetic absence epilepsy. Chaos **16**, 043111 (2006)
6. Sitnikova, E., Hramov, A.E., Grubov, V.V., Ovchinnkov, A.A., Koronovskii, A.A.: On–off intermittency of thalamo-cortical oscillations in the electroencephalogram of rats with genetic predisposition to absence epilepsy. Brain Res. **1436**, 147–156 (2012)
7. Rubchinsky, L., Park, C., Worth, R.: Intermittent neural synchronization in Parkinson's disease. Nonlinear Dyn. **68**(3), 329–346 (2012)
8. Krause, G., Elaskar, S., Riodel, E.: Type-I intermittency with discontinuous reinjection probability density in a truncation model of the derivative nonlinear Schrödinger equation. Nonlinear Dyn. **77**(3), 455–466 (2014)
9. Boccaletti, S., Valladares, D.L.: Characterization of intermittent lag synchronization. Phys. Rev. E **62**(5), 7497–7500 (2000)
10. Hramov, A.E., Koronovskii, A.A.: Intermittent generalized synchronization in unidirectionally coupled chaotic oscillators. Europhys. Lett. **70**(2), 169–175 (2005)
11. Moskalenko, O.I., Koronovskii, A.A., Shurygina, S.A.: Intermittent behavior on the boundary of the noise-induced synchronization. Tech. Phys. **56**(9), 1369–1372 (2011)
12. Pikovsky, A.S., Osipov, G.V., Rosenblum, M.G., Zaks, M., Kurths, J.: Attractor-repeller collision and eyelet intermittency at the transition to phase synchronization. Phys. Rev. Lett. **79**(1), 47–50 (1997)
13. Hramov, A.E., Koronovskii, A.A., Kurovskaya, M.K., Boccaletti, S.: Ring intermittency in coupled chaotic oscillators at the boundary of phase synchronization. Phys. Rev. Lett. **97**, 114101 (2006)
14. Popov, P.V.: Intermittent generalized synchronization in distributed autooscillatory media described by complex Ginzburg–Landau equations. Tech. Phys. Lett. **33**(9), 788–791 (2007)
15. Danilov, D.I., Koronovskii, A.A., Moskalenko, O.I.: Intermittency near the phase boundary of chaotic synchronization in spatially extended systems. Bull. Rus. Acad. Sci. Phys. **77**(12), 1460–1462 (2013)
16. Zhuravlev, M.O., Koronovskii, A.A., Moskalenko, O.I., Ovchinnikov, A.A., Hramov, A.E.: Ring intermittency near the boundary of the synchronous time scales of chaotic oscillators. Phys. Rev. E **83**, 027201 (2011)
17. Hramov, A.E., Koronovskii, A.A., Moskalenko, O.I., Zhuravlev, M.O., Ponomarenko, V.I., Prokhorov, M.D.: Intermittency of intermittencies. Chaos **23**(3), 033129 (2013)
18. Zhilin, Q., Gang, H.: Spatiotemporally periodic states, periodic windows, and intermittency in coupled-map lattices. Phys. Rev. E **49**(2), 1099–1108 (1994)
19. Kurths, J., Pikovsky, A.S.: Symmetry breaking in distributed systems and modulation spatio-temporal intermittency. Chaos Solitons Fractals **5**(10), 1893–1899 (1995)
20. Skoric, M.M., Jovanovic, M.S., Rajkovic, M.R.: Transition to turbulence via spatiotemporal intermittency in stimulated Raman backscattering. Phys. Rev. E **53**, 4056–4066 (1996)
21. Wang, X., Wang, M.: Projective synchronization of nonlinear-coupled spatiotemporal chaotic systems. Nonlinear Dyn. **62**(3), 567–571 (2010)
22. Godfrey, B.B.: Oscillatory nonlinear electron flow in Pierce diode. Phys. Fluids **30**, 1553 (1987)
23. Matsumoto, H., Yokoyama, H., Summers, D.: Computer simulations of the chaotic dynamics of the Pierce beam–plasma system. Phys. Plasmas **3**(1), 177 (1996)
24. Filatov, R.A., Hramov, A.E., Koronovskii, A.A.: Chaotic synchronization in coupled spatially extended beam–plasma systems. Phys. Lett. A **358**, 301–308 (2006)
25. Hramov, A.E., Koronovskii, A.A.: An approach to chaotic synchronization. Chaos **14**(3), 603–610 (2004)

26. Hramov, A.E., Koronovskii, A.A.: Time scale synchronization of chaotic oscillators. Phys. D **206**(3–4), 252–264 (2005)

27. Hramov, A.E., Koronovskii, A.A., Makarov, V.A., Pavlov, A.N., Sitnikova, E.: Wavelets in Neuroscience. Springer Series in Synergetics. Springer, London (2015)

28. Torresani, B.: Continuous Wavelet Transform. Savoire, Paris (1995)

29. Quiroga, R.Q., Kraskov, A., Kreuz, T., Grassberger, P.: Performance of different synchronization measures in real data: a case study on electroencephalographic signals. Phys. Rev. E **65**, 041903 (2002)

30. Koronovskii, A.A., Ovchinnikov, A.A., Hramov, A.E.: Experimental study of the time-scale synchronization in the presence of noise. Phys. Wave Phenom. **18**(4), 262–266 (2010)

31. Moskalenko, O.I., Phrolov, N.S., Koronovskii, A.A., Hramov, A.E.: Synchronization in the network of chaotic microwave oscillators. Eur. Phys. J. Special Topics **222**, 2571–2582(2013)

32. Hramov, A.E., Koronovskii, A.A., Popov, P.V., Rempen, I.S.: Chaotic synchronization of coupled electron-wave systems with backward waves. Chaos **15**(1), 013705 (2005)

33. Hramov, A.E., Koronovskii, A.A., Kurovskaya, M.K., Ovchinnikov, A.A., Boccaletti, S.: Length distribution of laminar phases for type-I intermittency in the presence of noise. Phys. Rev. E **76**(2), 026206 (2007)

34. Hramov, A.E., Koronovskii, A.A., Kurovskaya, M.K., Moskalenko, O.I.: Type-I intermittency with noise versus eyelet intermittency. Phys. Lett. A **375**, 1646–1652 (2011)

35. Moskalenko, O.I., Koronovskii, A.A., Zhuravlev, M.O., Hramov, A.E.: A discrete time model system with "intermittent" intermittency. Tech. Phys. Lett. **41**(1), 18–20 (2015)

36. Moskalenko, O.I., Koronovskii, A.A., Hramov, A.E., Zhuravlev, M.O., Levin, YuI: Cooperation of deterministic and stochastic mechanisms resulting in the intermittent behavior. Chaos Solitons Fractals **68**, 58–64 (2014)

37. Grebogi, C., Ott, E., Yorke, J.A.: Fractal basin boundaries, long lived chaotic transients, and unstable-unstable pair bifurcation. Phys. Rev. Lett. **50**(13), 935–938 (1983)